

Autoimmunity and effector recognition in *Arabidopsis thaliana* can be uncoupled by mutations in the RRS1-R immune receptor

Toby E. Newman^{1,3,*} (<https://orcid.org/0000-0001-5261-6104>), Jungmin Lee^{2,*}, Simon J. Williams⁴ (<https://orcid.org/0000-0003-4781-6261>), Sera Choi¹, Morgan K. Halane¹ (<https://orcid.org/0000-0001-6357-6232>), Jun Zhou³, Peter Solomon⁴ (<https://orcid.org/0000-0002-5130-7307>), Bostjan Kobe⁵ (<https://orcid.org/0000-0001-9413-9166>), Jonathan D.G. Jones⁶ (<https://orcid.org/0000-0002-4953-261X>), Cécile Segonzac^{7,8,§} (<https://orcid.org/0000-0002-5537-7556>) and Kee Hoon Sohn^{1,2,§} (<https://orcid.org/0000-0002-9021-8649>)

¹Department of Life Sciences, Pohang University of Science and Technology, Pohang 37673, Republic of Korea; ²School of Interdisciplinary Bioscience and Bioengineering, Pohang University of Science and Technology, Pohang 37673, Republic of Korea; ³Bioprotection Centre of Research Excellence, Institute of Agriculture and Environment, Massey University, Palmerston North 4442, New Zealand; ⁴Division of Plant Sciences, Research School of Biology, Australian National University, Acton, Australian Capital Territory 2601, Australia; ⁵School of Chemistry and Molecular Biosciences, Institute for Molecular Bioscience and Australian Infectious Diseases Research Centre, University of Queensland, Brisbane QLD 4072, Australia; ⁶The Sainsbury Laboratory, University of East Anglia, Norwich Research Park, Norwich NR4 7UH, United Kingdom; ⁷Department of Plant Science, Plant Genomics and Breeding Institute and Research Institute of Agriculture and Life Sciences, College of Agriculture and Life Sciences, Seoul National University, Seoul 08826, Republic of Korea. ⁸Plant Immunity Research Center, College of Agriculture and Life Sciences, Seoul National University, Seoul 08826, Republic of Korea.

This article has been accepted for publication and undergone full peer review but has not been through the copyediting, typesetting, pagination and proofreading process, which may lead to differences between this version and the Version of Record. Please cite this article as doi: 10.1111/nph.15617

This article is protected by copyright. All rights reserved.

§ Authors for correspondence:

Kee Hoon Sohn +82 54 279 2357 khsohn@postech.ac.kr,

Cécile Segonzac +82 2 800 2229 csegonzac@snu.ac.kr

Received: 16 July 2018

Accepted: 23 November 2018

*These authors contributed equally to this work.

SUMMARY

- Plant nucleotide-binding leucine-rich repeat (NLR) disease resistance proteins recognize specific pathogen effectors and activate a cellular defense program. In *Arabidopsis thaliana* (Arabidopsis) Resistance to *Ralstonia solanacearum* 1 (RRS1-R) and Resistance to *Pseudomonas syringae* 4 (RPS4) function together to recognize the unrelated bacterial effectors PopP2 and AvrRps4. In the plant cell nucleus, the RRS1-R/RPS4 complex binds to and signals the presence of AvrRps4 or PopP2.
- The exact mechanism underlying NLR signaling and immunity activation remains to be elucidated. Using genetic and biochemical approaches we characterized the intragenic suppressors of *sensitive to low humidity 1* (*slh1*), a temperature-sensitive auto-immune allele of *RRS1-R*.
- Our analyses identified 5 amino acid residues that contribute to RRS1-R^{SLH1} auto-activity. We investigated the role of these residues in the *RRS1-R* allele by genetic complementation and found that C15 in the TIR domain and L816 in the LRR domain were also important for effector recognition. Further characterization of the intragenic suppressive mutations located in the RRS1-R TIR domain revealed differing requirements for RRS1-R/RPS4-dependent autoimmunity and effector-triggered immunity.

- Our results provide novel information about the mechanisms that, in turn, hold an NLR protein complex inactive and allow adequate activation in the presence of pathogens.

Key words: Arabidopsis, autoimmunity, immune receptor complex, paired nucleotide-binding leucine-rich receptors (NLRs), Toll/interleukin-1 receptor (TIR) domain

INTRODUCTION

Unlike animals that possess an adaptive immune system of mobile defender cells, the plant innate immune system is inborn and multi-layered, dependent on individual cells sensing pathogen presence and subsequently triggering an immune response. The initial layer of plant immunity is activated upon recognition of pathogen-associated molecular patterns (PAMPs) via cell surface-localized pattern recognition receptors. This results in pattern-triggered immunity (PTI), a defense-signaling pathway that induces a multitude of cellular changes to prevent pathogen proliferation (Boutrot and Zipfel, 2017). This basal defense response can be overcome by successful pathogens through secretion of immunity-dampening proteinaceous effectors. Plants have, however, evolved disease resistance genes (*R*), the products of which recognize specific pathogen effectors and activate an amplified defense response termed effector-triggered immunity (ETI). This often culminates in the hypersensitive response (HR), a form of localized programmed cell death (Jones and Dangl, 2006). In reality, the dichotomy between PAMPs and effectors and, similarly, PTI and ETI is not always so clearly defined; however, detection of pathogen invasion by host receptors is essential (Cook et al., 2015).

R genes typically encode nucleotide-binding (NB) domain and leucine-rich repeat (LRR) containing (NLR) receptors. NLRs recognize intracellular pathogen effectors either directly through physical association or, more commonly, indirectly via the detection of modification of host proteins. Activation of the NLR proteins results in a strong defense response that restricts pathogen growth. As the defense responses are energetically costly and can impair growth, plants avoid inappropriate NLR activation. In the absence of the matching effector(s), NLRs exist in an inactive, auto-inhibited state maintained through interactions within the NLR modular structure. The N-terminal Toll/interleukin-1 receptor (TIR) or

coiled-coil (CC) domains of plant NLRs are involved in downstream signaling. Indeed, there are several examples of TIR or CC domains eliciting an HR-like cell death response when ectopically expressed *in planta* (Zhang et al., 2017a). It is thought that a main function of the LRR domain is in auto-inhibition of the NLR activity, although other roles such as direct effector binding have also been demonstrated (Dodds et al., 2006; Ade et al., 2007; Schreiber et al., 2016). The NB domain is also responsible for maintaining an inhibited state through ADP binding. ADP/ATP exchange by the NB domain results in a conformational switch to the active state (Takken and Tameling, 2009).

Several studies over the years have helped to decode how NLRs are kept in an 'off' state, mainly through forward genetic screens which have led to the identification of autoimmune-suppressed Arabidopsis mutants. For example, *snc1* (*suppressor of npr1-1, constitutive 1*) is a gain-of-function mutant caused by a point mutation between the NB and LRR encoding regions of the TIR-NB-LRR (TNL) *SNC1* gene (Li et al., 2001). This mutation results in an over-accumulation of SNC1 protein and subsequent autoimmunity associated with severe growth retardation (Zhang et al., 2003). Forward-genetic screens to identify suppressors of *snc1* autoimmunity resulted in the discovery of several key players of TNL regulation (Johnson et al., 2012). However, it is unclear if these components are required for specific ETI signaling as the pathogen effector recognized by SNC1 is still unknown.

The majority of NLRs function individually to recognize an effector and signal to activate immune mechanisms; however, some NLRs function cooperatively in a dual NLR complex, as demonstrated in rice for the paired RGA4/RGA5 and Pi5-1/Pi5-2 CC-NB-LRR (CNL) genes, which confer resistance to *Magnaporthe oryzae* (Lee et al., 2009; Cesari et al., 2014a). In Arabidopsis, the best-studied case is the TNL pair formed by *RRS1-R* (*RESISTANCE TO RALSTONIA SOLANACEARUM 1*) and *RPS4* (*RESISTANCE TO PSEUDOMONAS SYRINGAE 4*). *RRS1-R* is thought to act as a sensor NLR that perceives the effector(s), while *RPS4* acts as the signaling NLR to activate a defense response (Le Roux et al., 2015; Sarris et al., 2015). The pathogen effectors target or modify the WRKY DNA-binding domain of *RRS1-R*, which suggests that the integrated WRKY domain is a decoy for effectors targeting *bona fide* WRKY transcription factors (Cesari et al., 2014b; Le Roux et al., 2015; Sarris et al., 2015). Protein-protein interaction data have clarified how *RRS1-R* and *RPS4* function to trigger immunity. Structure/function analyses of *RRS1-R/RPS4* show that their TIR domains bind to each other directly and identified the corresponding interaction interfaces (Williams et al., 2014). Interestingly, although *RRS1-R* and *RPS4* TIR domains

self-associate to form homodimers using the same TIR interfaces identified in the heterodimer, they form a heterodimer with a much higher affinity. Importantly, RRS1-R TIR domain binding to RPS4 TIR domain suppresses the signaling activity of RPS4 in the absence of corresponding effectors, suggesting immune activation involves dissociation of this heterodimeric interaction (Bernoux et al., 2011; Williams et al., 2014; Zhang et al., 2017b).

RPS4 and RRS1-R were originally hypothesized to function independently for the recognition of two sequence-unrelated bacterial effectors, AvrRps4 and PopP2, respectively, but have since been shown to function cooperatively (Birker et al., 2009; Narusaka et al., 2009; Sohn et al., 2014). More recently, a second NLR pair homologous to RRS1-R and RPS4, RRS1B and RPS4B, was shown to confer recognition of AvrRps4 but not PopP2 (Saucet et al., 2015). Intriguingly, inappropriate pairing of RRS1-R/RPS4B or RPS4/RRS1B fails to activate AvrRps4-triggered immunity, highlighting the specificity of these pairs in activating immunity. However, TIR domain swaps in chimeric protein between RRS1-R and RRS1B and RPS4 and RPS4B retain immunocompetence, implying that other regions of the proteins outside of the TIR domains account for this specificity.

An autoimmune mutant of *RRS1-R* was identified that harbors a single leucine insertion in the RRS1-R WRKY DNA-binding domain (Noutoshi et al., 2005). This mutant allele, *slh1* (*sensitive to low humidity 1*), confers temperature-sensitive constitutive defense activation, resulting in a severely stunted morphology. A forward genetic screen identified *suppressor of slh1 immunity* (*sushi*) mutants, which display a range of recovered growth (Sohn et al., 2014). More than half of the characterized *sushi* carry causal mutations in the coding sequence of *RPS4*, demonstrating the striking similarity between *slh1*-induced defense responses and RRS1-R/RPS4-dependent effector recognition and subsequent immunity. Characterization of *RPS4*^{SUSHI} variants also helped to unravel the complex features of interaction between RPS4 and RRS1-R. To expand our knowledge of the intricate function of this NLR pair, we undertook the characterization of the alleles of the second most abundant class of *sushi*, which harbor mutations in the coding sequence of *RRS1-R*.

In this study, we identified 5 causal intragenic *RRS1-R SUSHI* mutations, which at least partially restored stunted morphology and suppressed defense gene upregulation in *slh1*. The *SUSHI* mutations differentially affected auto-activity and effector recognition functions of RRS1-R, as demonstrated by complementation of the *rrs1 rrs1B* Arabidopsis mutant. We

could further show that the C15Y mutation in the TIR domain abolishes RRS1-R function by disrupting heterodimer formation with its signaling partner, RPS4. Importantly, we demonstrate that several *SUSHI* mutations abolish autoimmunity but not effector-triggered immunity. Finally, we generated RRS1B variants harboring corresponding *SUSHI* mutations, which highlights intriguing differences between RRS1-R and RRS1B TIR domain function, particularly in keeping the immune complex inactive.

MATERIALS & METHODS

Plant materials and growth conditions

Arabidopsis plants were grown in short day conditions (11 h : 13 h, light: dark) at 22°C. *Nicotiana benthamiana* and *Nicotiana tabacum* W38 plants were grown in long-day conditions (14 h : 10 h, light : dark) at 25°C. No-0 and *slh1* were described in (Noutoshi et al., 2005); *Ws-2 rrs1-1* was described in (Narusaka et al., 2009); Col-0 *rrs1-3 rrs1B-1* was described in (Saucet et al., 2015).

Plasmid constructions

Genes were amplified with gene-specific primers, which introduced flanking *BsaI* recognition sequences and specific 4 base-pair (bp) overhangs. These were ligated into the pICH41021 shuttle vector (modified pUC19 with a mutated *BsaI* recognition sequence). Subsequently, pICH41021 constructs were assembled into the appropriate Golden Gate-compatible destination vector with an epitope tag (Engler et al., 2008).

To generate the constructs for floral dip transformation of *rrs1-3 rrs1B-1*, the *RRS1-R* (*Ws-2*) gene was amplified in 3 modules (2016 bp, 2536 bp and 1728 bp respectively) using the oligonucleotide primers listed in Table S1. To introduce polymorphisms, site-directed mutagenesis was performed on the appropriate modules (Table S1). These modules were subsequently assembled with the RRS1-R native promoter and a C-terminal 3xFlag tag into a Golden Gate-compatible vector, pEpiGreenB5.

For *Agrobacterium*-mediated delivery of constructs into *N. tabacum* and *N. benthamiana*, the Golden Gate-compatible binary vector, pICH86988 (provided by Sylvestre Marillonnet), was utilized. Gene variants were fused to a C-terminal epitope tag and assembled into pICH86988. Effectors *avrRps4* and *popP2* were fused to a C-terminal YFP tag, *RRS1-R* (from Ws-2) and *RRS1B* (from Col-0) variants were fused to a C-terminal 3xFLAG tag, *RPS4* was fused to a C-terminal 6xHA tag, *RRS1-R* and *RRS1B* TIR variants were fused to a C-terminal YFP tag and *RPS4* TIR was fused to a GFP tag.

For Yeast-two hybrid (Y2H) assays, Golden Gate-compatible pLexA-DBD and pB42-AD vectors were used. The *RPS4* TIR coding sequence (CDS) was fused to C-terminal 3xFLAG and cloned into the pLexA-DBD vector; *RRS1-R* TIR CDS variants were fused to C-terminal 6xHA and cloned into the pB42-AD vector. The TIR domain sequences were cloned from Arabidopsis cDNA (Ws-2 accession).

Plant pathology experiments

For hypersensitive response (HR) assays in Arabidopsis, *Pseudomonas fluorescens* Pf0-1(T3S) strains were streaked from glycerol stocks onto King's B plate with antibiotic selection and incubated for two days at 28°C. Bacteria harvested from plates were re-suspended in 10 mM MgCl₂ and diluted to OD₆₀₀ = 0.2 for HR assays. Bacterial suspensions were infiltrated into the abaxial surface of 5-week old Arabidopsis leaves using a blunt-end syringe. HR was observed and photographed at 18 to 24 hours post infiltration (hpi).

For bacterial growth assays in transgenic lines, *Pseudomonas syringae* pv. *tomato* (*Pto*) DC3000 strains were streaked and re-suspended as for HR assays and diluted to OD₆₀₀ = 0.001 for bacterial growth assays (Sohn et al., 2014). Bacterial suspensions were infiltrated as for HR assays and at 4 dpi, leaf discs were taken and ground in sterile 10 mM MgCl₂. Each sample was serially diluted in sterile 10 mM MgCl₂ and 20 µL spots of each sample (n = 6) and dilution were plated on King's B plates with appropriate antibiotics. After 2 days incubation at 28°C the colony forming unit (CFU) were counted for the least dilute sample possible.

Yeast-two-hybrid assays

For Y2H assays, *Saccharomyces cerevisiae* strains EGY48 Mat(α) and RFY206 Mat(a) were used. The latter carries the pSH18-34 vector which encodes the lacZ reporter gene under the control of 8 upstream LexA operators and the URA3 selectable marker, allowing growth on media lacking uracil. EGY48 and RFY206 (pSH18-34) were transformed with pB42-AD and pLexA-DBD constructs, respectively, using the 'Frozen-EZ Yeast Transformation II Kit' according to the manufacturer's recommendations (Zymo Research). pB42-AD encodes the TRP1 selectable marker, which allows yeast growth on media lacking tryptophan (Trp), pLexA encodes the HIS3 selectable marker, allowing growth on media lacking histidine (His). After transformation of yeast with the appropriate constructs, mating and interaction assays were performed as described in the Yeast Protocols Handbook (Clontech).

Agrobacterium*-mediated stable transformation of *Arabidopsis thaliana

Arabidopsis thaliana rrs1-3 rrs1B-1 plants were transformed using the floral dip transformation method described by Clough and Bent (1998) with *Agrobacterium tumefaciens* AGL1 carrying pEpiGreenB5 with *RRS1-R* variants. Transgenic plants were selected using the phosphinotricin at 50 $\mu\text{g}\cdot\text{mL}^{-1}$ and two independent T2 lines were selected for each genotype.

Agrobacterium*-mediated transient transformation of *Nicotiana benthamiana* and *Nicotiana tabacum

Agrobacterium tumefaciens AGL1 carrying the binary constructs were grown in liquid L-medium supplemented with the appropriate antibiotics for 24 h. Cells were harvested by centrifugation and re-suspended in infiltration medium (10 mM MgCl_2 and 10 mM MES pH 5.6). Suspensions were then adjusted to $\text{OD}_{600} = 0.1-0.4$. Bacterial suspensions were mixed in a 1:1 ratio and infiltrated into the abaxial surface of 5-week old *N. benthamiana* or *N. tabacum* leaves using a blunt-end syringe. Cell death was observed and photographed after 2 to 3 dpi.

Protein extraction, immunopurification and immunoblotting

Plant protein samples were prepared from *N. benthamiana* 36 h after agro-infiltration. One fully infiltrated leaf was ground in liquid nitrogen and total proteins were extracted in GTEN buffer (10% glycerol, 150 mM Tris-HCl pH 7.5, 1 mM EDTA, 150 mM NaCl) supplemented with 5 mM DTT, protease inhibitor cocktail tablet (cOmplete, Roche) and 0.2% (vol/vol) Nonidet P-40. Lysates were centrifuged for 15 min at 2500 g at 4°C. Supernatants were filtered through a fine mesh (Miracloth, Millipore) and used as input samples.

Immunoprecipitations were conducted on 1.5 mL of filtered extract incubated for 2 h at 4°C under gentle agitation in presence of 15 µL anti-FLAG M2 affinity gel (Sigma). Antibodies-coupled agarose beads were collected and washed three times in GTEN buffer, re-suspended in SDS-loading buffer and denatured 10 min at 96°C. Proteins were separated by SDS-PAGE and analyzed by immunoblotting using anti-FLAG M2-HRP (Sigma), anti-GFP-HRP (Santa Cruz) or anti-HA antibodies (Roche). Proteins were detected with a mix of SuperSignal West Pico and SuperSignal West Femto chemiluminescent substrates (Pierce). Membranes were stained with Ponceau S (Sigma) to visualize protein loading.

RNA extraction and quantitative RT-PCR

Total RNAs were extracted from 4 to 5 week-old Arabidopsis plants using the TRI reagent (Invitrogen) according to the manufacturer's instructions. First-strand cDNA was synthesized from 5 µg RNA using Maxima First Strand cDNA synthesis kit (ThermoFisher Scientific) and an oligo(dT) primer, according to the manufacturer's instructions. cDNA was amplified in triplicate by quantitative PCR using Prime Q-master mix (Genet Bio) and the StepOnePlus RT-PCR cycler (ThermoFisher Scientific). The relative expression values were determined using the comparative Ct method and *Ef1α* (*At5g60390*) as reference. Primers used for quantitative PCR are described in Table S1 (Sohn et al., 2014).

Recombinant protein production, circular dichroism spectroscopy and protein-protein interaction assay

The C15Y and P68L mutations were introduced into RRS1-R(6-153) within the pMCSG7 vector (Wan et al., 2013) by site-direct mutagenesis using the primers described in Table S1. Protein expression and purification of RPS4(10-178) and RRS1-R(6-153) were performed as described previously (Wan et al., 2013). RRS1-R(6-153)^{C15Y} and RRS1-R(6-153)^{P68L} were expressed and purified under the conditions used for RRS1-R(6-153); RRS1-R(6-153)^{C15Y} behaved largely like the wild-type protein; however, RRS1-R(6-153)^{P68L} could not be produced in a soluble form. Circular dichroism (CD) spectroscopy was used to compare the secondary structure of RRS1-R(6-153) and the RRS1-R(6-153)^{C15Y}. Far-UV CD spectra were collected from 197 to 260 nm using a Chirascan spectrometer. Samples containing 0.05 mg mL⁻¹ of purified protein were measured at room temperature with a 1 mm cuvette, 1.0 nm bandwidth and 0.5 s integration time. Three scans were averaged, and the spectra were corrected for buffer baseline contribution. The data was visualised using the webserver CAPITO (<http://capito.nmr.leibniz-fli.de/>) (Wiedemann et al., 2013) with data smoothing selected. Protein-protein interaction was tested using a SuperdexTM 75 Increase 10/300 GL size-exclusion chromatography (SEC) column (GE Healthcare). For single reactions, 100 µL containing 60 µg of RPS4(10-178) and 50 µg of RRS1-R(6-153) and RRS1-R(6-153)^{C15Y} was separated over the column. For protein-protein interactions, 60 µg of RPS4(10-178) was combined with 50 µg of RRS1-R(6-153) or RRS1-R(6-153)^{C15Y} and incubated on ice for 1 hour prior to separation over the SEC column.

RESULTS

Identification of intragenic suppressors of RRS1-R^{SLH1}-mediated immunity.

To gain insights into the mode of activation of the RRS1-R/RPS4 immune complex, we previously conducted a genetic screen and identified suppressors of *slh1*-mediated immunity (*sushi*). Among the 72 *sushi* lines descending from plants homozygous for the *slh1* mutation that grew and set seeds at the permissive temperature of 22°C, 46 carry a single nucleotide change in the *RPS4* coding sequence (Sohn et al., 2014). Here, we identified 12 *sushi* mutants that carry a nonsense or missense polymorphism in the *RRS1-R* TIR (3 lines), NB (4 lines) or LRR (5 lines) domain coding sequence and further characterized some of them (Table 1).

Similar to M2 generation, we observed in the M3 generation that plants carrying the homozygous *SUSHI* mutation in *RRS1-R^{SLH1}* displayed significant recovery from the *RRS1-R^{SLH1}*-dependent lethal phenotype (Fig. 1a). We observed improved morphology and development of these *sushi* mutants compared to *slh1*, ranging from very partial recovery in *sushi45* and *sushi26* to quasi-WT morphology in *sushi84* and *sushi88*. The extremely stunted growth of *slh1* stems from temperature-dependent constitutive activation of *RRS1-R^{SLH1}*-dependent immunity signaling and elevated expression of defense-related genes (Noutoshi et al., 2005; Sohn et al., 2014). In order to investigate if enhanced growth of *sushi* mutants compared to *slh1* correlates with reduced defense gene expression, we tested expression of several genes whose expression is markedly upregulated during *RRS1-R*-dependent ETI (Sohn et al., 2014). In plants grown at a non-permissive temperature (28°C), expression of the defense-marker genes *FMO1*, *PBS3* and *PR1* is barely detectable in No-0, *slh1* and the 6 *sushi* lines (Fig. 1b). However, upon shifting plants to a permissive temperature (19°C), expression of the 3 marker genes was remarkably elevated in *slh1*, while not affected in No-0, *sushi84*, *sushi23* and *sushi88*. We could, however, detect a slight induction of *FMO1*, *PBS3* and *PR1* expression in *sushi45*, *sushi11* and *sushi26*, although to a much lesser extent than that observed in *slh1*. These results indicate that the rescued morphology observed in the 6 *sushi* lines was associated with suppression of defense signaling.

***SUSHI* mutations in *RRS1-R* cause suppression of *slh1*-mediated immunity.**

According to previous findings, *RRS1-R* or *RRS1-R^{SLH1}* can function only when in the homo- or hemizygous but not the heterozygous state (Deslandes et al., 2002; Noutoshi et al., 2005). To confirm that the identified missense mutations in the *RRS1-R* coding sequence are indeed the cause of the suppressed *slh1* lethality, we crossed the 6 *sushi* mutants and WT No-0 to the Ws-2 *rrs1-1* knock-out mutant. If intragenic *SUSHI* mutations identified in *RRS1-R^{SLH1}* are causal, F₁ hybrids would show quasi-WT morphology. F₁ hybrids descending from these crosses were confirmed hemizygous at the *RRS1-R* locus (*RRS1-R^{SLH1/sushi}/rrs1*) using the *slh1* genotyping CAPS marker (Noutoshi et al., 2005) (Fig. S1). When grown at the permissive temperature (22°C), 5 of the *sushi* x *rrs1-1* F₁ hybrids displayed a morphology similar to that of the No-0 x *rrs1* hybrid, demonstrating that the respective missense mutations in the *RRS1-R* coding sequence caused the suppression of *slh1* lethality (Fig. 2a). On the other hand, we could infer from the stunted growth of the *sushi23* x *rrs1* F₁ hybrids

that the corresponding change in *RRS1-R* is insufficient to suppress the *slh1* lethality.

Defense-related gene expression in these hybrids mostly correlated with their morphology (Fig. 2b). *FMO1*, *PBS3* and *PR1* expression was elevated in *sushi23* x *rrs1* small hybrid plants compared with the other *sushi* x *rrs1* hybrids. We can, therefore, hypothesize that *sushi23* harbors a second mutation at an unknown locus encoding a component of RRS1-R^{SLH1} signaling. Of note, we measured a slightly elevated *FMO1* expression in *sushi45* x *rrs1* and *sushi11* x *rrs1* F₁ hybrids, which may indicate a residual activity of the *RRS1-R*^{SLH1} allele in these plants. Notwithstanding, this analysis revealed 5 amino acid substitutions in RRS1-R that led to suppression of aberrant defense responses in the *slh1* mutant.

Single amino acid changes in RRS1-R differentially affect autoimmunity and effector-triggered immunity.

To examine whether the 5 substitutions that suppress RRS1-R^{SLH1}-mediated immunity could also impact RRS1-R effector recognition function, we introduced each of the *SUSHI* mutations in the Ws-2 *RRS1-R* allele, which confers recognition of AvrRps4 and PopP2 (Birker et al., 2009; Narusaka et al., 2009; Sohn et al., 2014) (Fig. S2). Note that the No-0 RRS1-R L814 residue aligns with L816 in Ws-2 RRS1-R due to a two amino acid insertion in Ws-2 RRS1-R exon 4 (Table 1, Fig. S2). We transformed these constructs in the *rrs1 rrs1B* Col-0 background to exclude the contribution of RRS1B/RPS4B to AvrRps4 recognition from our analysis (Saucet et al., 2015) (Fig. 3a). We then observed the hypersensitive response (HR) in selected T2 plants expressing RRS1-R variants infiltrated with modified *Pseudomonas fluorescens* Pf0-1 carrying type III secretion system (hereafter, Pf0-1(T3S)) and carrying empty vector (EV), *avrRps4* or *popP2* (Sohn et al., 2014; Thomas et al., 2009) (Fig. 3b). As expected, both effectors triggered HR in Ws-2 ecotype naturally expressing RRS1-R but not in the *rrs1 rrs1B* mutant. The transgenic *rrs1 rrs1B* plants expressing RRS1-R^{WT} displayed HR in response to Pf0-1(T3S)-delivered AvrRps4 or PopP2. Strikingly, both effectors also triggered HR in the transgenic *rrs1 rrs1B* expressing RRS1-R^{P68L}, RRS1-R^{G176E} or RRS1-R^{C607Y}, while they could not in the plants expressing RRS1-R^{C15Y} or RRS1-R^{L816F}.

To further investigate the role of *SUSHI* mutations in AvrRps4- or PopP2-triggered immunity, we also measured the multiplication of the virulent *Pseudomonas syringae* pv. *tomato* (*Pto*) DC3000 strain carrying EV, *avrRps4* or *popP2* in the *rrs1 rrs1B/RRS1-R*^{*sushi*} transgenic lines (Fig. 3c). Effector recognition by RRS1-R in transgenic *rrs1 rrs1B/RRS1-*

R^{WT} plants led to a significant (>10-fold) reduction of avirulent *Pto* DC3000 growth compared with *rrs1 rrs1B*. Consistent with our HR assay results, we observed a similar growth restriction of avirulent strains in the *rrs1 rrs1B* transgenic plants expressing RRS1-R^{P68L}, RRS1-R^{G176E} or RRS1-R^{C607Y}. Conversely, *Pto* DC3000 (AvrRps4) and *Pto* DC3000 (PopP2) multiplied to a similar level as *Pto* DC3000 (EV) in *rrs1 rrs1B/RRS1-R*^{C15Y} and *rrs1 rrs1B/RRS1-R*^{L816F} lines. In summary, these experiments revealed that although all 5 *SUSHI* mutations were confirmed as suppressors of RRS1-R^{SLH1}-mediated autoimmunity, P68L, G176E and C607Y do not abolish effector-triggered RRS1-R-mediated immunity.

C15Y but not L816F significantly reduces RRS1-R interaction with RPS4.

RRS1-R forms an immunocompetent complex in association with RPS4 to recognize AvrRps4 and PopP2 (Williams et al., 2014; Sohn et al., 2014; Sarris et al., 2015). To further characterize the effect of the *SUSHI* mutations on RRS1-R protein function, we therefore tested the interaction of RRS1-R^{SUSHI} variants with RPS4 by co-immunoprecipitation. Flag-tagged RRS1-R, WT or carrying the *SUSHI* mutations, were transiently co-expressed with HA-tagged RPS4 in *Nicotiana benthamiana* (Fig. 4). In agreement with previous data (Sohn et al., 2014; Williams et al., 2014), RRS1-R associated with RPS4 *in vivo*. Interestingly, RRS1-R^{C15Y} showed greatly reduced association with RPS4 whereas RRS1-R^{L816F}, the other variant that affected effector recognition, could associate with RPS4 in a manner similar to RRS1-R^{WT}. Likewise, the P68L, G176E, C607Y and P741L changes did not affect the ability of RRS1-R to associate with RPS4. These results indicate that although both C15Y and L816F cause changes in RRS1-R effector recognition, only the C15Y mutation affects the formation of the RRS1-R/RPS4 complex *in vivo*.

C15Y or P68L mutations in the RRS1-R TIR domain significantly reduce suppression of RPS4 TIR domain-mediated cell death and interaction with the RPS4 TIR domain.

The N-terminal region of RPS4 (amino acids 1 to 236) comprising the TIR domain and a short stretch of the NB domain, induces effector-independent cell death when transiently over-expressed in tobacco (Swiderski et al., 2009; Zhang et al., 2004). RPS4 TIR domain-mediated cell death can be suppressed by co-expression with the RRS1-R TIR domain (amino acids 1 to 175) (Williams et al., 2014). This suppression requires the SH motif that is

located at the TIR-TIR domain interface (Williams et al., 2014). We therefore tested whether the 2 *SUSHI* mutations, C15Y and P68L, located in the RRS1-R TIR domain could affect the RPS4 TIR domain-mediated cell death (Fig. 5a). Similar to RRS1-R(1-175)^{WT} and RRS1-R(1-175)^{S25A/H26A}, *Agrobacterium*-mediated transient expression (hereafter, agro-infiltration) of RRS1-R(1-175)^{C15Y} or RRS1-R(1-175)^{P68L} alone did not induce cell death (Williams et al., 2014) (Fig. 5b). As expected, agro-infiltration of RPS4(1-236) with GFP or RRS1-R(1-175)^{S25A/H26A} but not with RRS1-R(1-175)^{WT} induced a cell-death response. Interestingly, co-expression with RRS1-R(1-175)^{C15Y} or RRS1-R(1-175)^{P68L} also failed to suppress RPS4(1-236)-mediated cell death (Fig. 5b). This result suggests that C15 and P68 are required for the inhibitory activity of the RRS1-R TIR domain on RPS4 TIR domain-mediated defense activation.

Because RRS1-R and RPS4 TIR domains physically associate with each other, we examined the effect of C15Y and P68L on the direct physical interaction between RPS4 and RRS1-R TIR domains. To this end, we used a LexA-based yeast-two-hybrid (Y2H) system where RPS4(1-236) was fused to the LexA DNA-binding domain, and RRS1-R(1-175) variants were fused to the B42 activation domain (Fig. 5c). As previously reported (Williams et al., 2014), RPS4(1-236) physically interacts with RRS1-R(1-175)^{WT} but not with RRS1-R(1-175)^{S25A/H26A} in yeast cells. We also observed a lack of interaction between the RPS4 TIR domain and RRS1-R(1-175)^{C15Y} or RRS1-R(1-175)^{P68L}, although all the RRS1-R TIR domain variants accumulated to a similar amount in yeast cells.

Previously, we have shown that purified forms of the RPS4 and RRS1-R TIR domains produced in *Escherichia coli* form a stable 1:1 heterodimeric complex (Williams et al., 2014). To test the effect of the C15Y and P68L mutations on this interaction *in vitro*, we expressed RRS1-R(6-153)^{C15Y} and RRS1-R(6-153)^{P68L} in *E. coli*. However, despite multiple attempts, only the C15Y mutant could be produced and purified in a soluble form, with similar yields to the wild-type protein (Fig. 5e). In addition, circular dichroism (CD) spectroscopy of the purified RRS1-R(6-153) and RRS1-R(6-153)^{C15Y} proteins revealed very similar spectra, indicative of folded, predominantly helical proteins (Fig. 5d and e) (Wan et al., 2013). As previously reported (Williams et al., 2014), RRS1-R(6-153) and RPS4(10-178) recombinant proteins formed a complex over size-exclusion chromatography, consistent with the heterodimer as evident by the earlier elution profile (Fig. 5f). However, RRS1-R(6-153)^{C15Y} failed to form a complex with RPS4(10-178), indicating that this mutation abolishes the TIR-TIR interaction (Fig. 5f). Taken together, these data suggest that RRS1-R TIR domain

carrying C15Y or P68L mutation loses the ability to suppress RPS4 TIR domain-mediated defense activation due to reduced TIR-TIR association.

C12Y and P63L mutations do not affect RRS1B function.

The Arabidopsis genome contains close homologs of *RRS1-R* and *RPS4*, *RRS1B* and *RPS4B*, which are 60% identical to *RRS1-R* and *RPS4*, and also genetically and physically associate with each other to recognize AvrRps4 (Saucet et al., 2015). Although incorrect pairing (e.g. *RRS1B/RPS4* or *RRS1-R/RPS4B*) leads to non-functional complexes, TIR domain swaps between these two protein pairs retain effector recognition function. This suggests that the TIR domains have similar roles for effector-triggered activation in both paired NLRs (Saucet et al., 2015). *RRS1B* and *RRS1-R* TIR domains share ~70% identity at the amino acid level and the S25H26 motif (S22H23), C15 (C12) and P68 (P63) residues are located in highly conserved regions of *RRS1-R* and *RRS1B*, respectively (Fig. S3). Therefore, we sought to examine whether these residues are equally important for *RRS1B* function, using the well-established agro-infiltration assay system in tobacco (Sohn et al., 2014; Sarris et al., 2015; Saucet et al., 2015). Co-expression of *RPS4* and *RRS1-R*^{WT} but not *RRS1-R*^{S25AH26A} with AvrRps4 or PopP2 led to cell death (Fig. 6a). Consistent with the data obtained in Arabidopsis transgenic lines (Fig. 3), *RRS1-R*^{P68L} but not *RRS1-R*^{C15Y} could recognize the effectors when co-expressed with *RPS4*. As previously shown (Saucet et al., 2015), co-expression of *RPS4B* and *RRS1B*^{WT} with AvrRps4 also led to cell death in tobacco leaves (Fig. 6b). However, while this signaling was dependent on the S22H23 motif, the C12Y and P63L substitutions did not affect *RRS1B/RPS4B*-mediated recognition of AvrRps4. This result indicated that only the SH motif was required for activation of the *RRS1B/RPS4B* complex by AvrRps4 recognition. It was demonstrated that, similar to the *RRS1-R* TIR domain, the *RRS1B* TIR domain can suppress *RPS4*(1-236)-mediated cell death in tobacco (Saucet et al., 2015). Consistent with this previous finding, *RRS1B*(1-166) suppressed *RPS4*(1-236)-mediated cell death in tobacco (Fig. 6c). Surprisingly, this suppression was still effective when *RPS4*(1-236) TIR domain was co-expressed with *RRS1B*(1-166)^{S22A/H23A}, *RRS1B*(1-166)^{C12Y} or *RRS1B*(1-166)^{P63L} TIR domain (Fig. 6c). Full-length or truncated *RRS1B* variants showed detectable protein expression level by immunoblot analysis (Fig. S4). Taken together, our results revealed the distinct requirements of *RRS1B* TIR domain function in effector recognition in comparison to the *RRS1-R* TIR domain.

DISCUSSION

We report the identification of several missense and nonsense *SUSHI* mutations in RRS1-R that abolish autoimmunity of RRS1-R^{SLH1}. Unexpectedly, three of these *SUSHI* mutations (P68L, G176E and C607Y) did not alter RRS1-R/RPS4-mediated recognition of the corresponding effectors AvrRps4 and PopP2. Detailed analysis of C15Y and P68L changes in the RRS1-R TIR domain revealed that the P68L mutation reduced heterodimeric TIR-TIR association between RRS1-R and RPS4, but did not significantly alter the interaction of full-length proteins. These results may suggest that the RRS1-R TIR domain carries a property that is dispensable for effector recognition but essential for autoimmunity. On the other hand, the corresponding mutations in RRS1B, C12Y and P63L, did not alter AvrRps4 recognition. This may indicate that mechanistically distinct properties are required for activation of functionally redundant (for AvrRps4 recognition) NLRs, RRS1-R and RRS1B.

The TIR domain plays a crucial role in NLR activation of plant immunity. TIR domain-induced initiation of HR was first demonstrated over a decade ago in the flax NLR L10 and Arabidopsis RPS4 studied herein (Frost et al., 2004; Zhang et al., 2004). The downstream signaling cascade that culminates in HR is initiated upon proper TIR-TIR domain self-association, such as in flax L6 (Bernoux et al., 2011). Interestingly, it appears that TIR domains from different NLRs may employ a common self-association mechanism via multiple interfaces (Zhang et al., 2017b; Nishimura et al., 2017).

Similarly, TIR-TIR domain heterodimeric association is a fundamental requirement for paired NLR function. However, this TIR-TIR domain association is not only involved in the induction of HR but can also be involved in auto-inhibition of the immune complex. Williams et al. (2014) showed that the defense induction mediated by RPS4 TIR domain self-association is repressed in the resting state by heterodimerization of the RPS4 TIR domain with the RRS1-R TIR domain. This revealed a new layer of function for TIR domain association other than downstream signaling. A similar yet distinct mechanism has been demonstrated in the paired RGA4 and RGA5 via their CC domains (Cesari et al., 2014a).

Despite the RRS1-R TIR domain repressing RPS4 TIR domain-mediated cell death, RRS1-R/RPS4 TIR-TIR domain interaction is crucial for the effector recognition function of this NLR pair (Williams et al., 2014). Our findings here corroborate this and shed more light on the molecular basis of proper immune complex formation. Two RRS1-R TIR domain mutations, C15Y and P68L, were identified as causal *SUSHI* mutations and were shown to

impair association with the RPS4 TIR domain. Therefore, the role of the RRS1-R TIR domain in this system is not simply to maintain auto-inhibition. In the full-length context, proper association of the RRS1-R TIR domain with the RPS4 TIR domain may be required to transmit the signal from the effector sensor (RRS1-R) to the signal transducer (RPS4).

With reference to the RRS1-R TIR domain structure, C15 resides within the β A strand and is not surface-exposed, while P68 is surface-exposed at the C-terminus of the β C strand. In the RRS1-R/RPS4 TIR domain heterodimeric structure, neither C15 nor P68 localize to the protein-protein interface; therefore, understanding the causal effect of the mutation that results in the loss of TIR-TIR domain interaction is not trivial. One explanation for the loss of interaction between RPS4 and RRS1-R C15Y is that the substitution of a bulky tyrosine side-chain at this position would cause a clash with residues located on the α A helix (Fig. S5). The α A helix is critical for both hetero- and homomeric interactions in TIR domains (Williams et al., 2014; Zhang et al., 2017b). As such, the C15Y mutation may have an indirect effect on the interface, because some repositioning of the α A helix could be required to compensate for the mutation, and this may in turn be destabilizing to the interaction interface. Despite this, the mutation itself is tolerated in terms of folding of the TIR domain in *E. coli*, as the CD spectra of the wild-type and mutant proteins are essentially indistinguishable. Conversely, soluble forms of the P68L mutant could not be produced in this recombinant system. One possible explanation of these data is that the P68L mutation has a disruptive effect on the overall structure and fold of the TIR domain; however, given the heterologous nature of its production, other factors cannot be discounted. The RRS1-R P68L TIR domain does accumulate in yeast, although this is not necessarily an indicator of a properly folded protein. It is plausible that in the context of the full-length RRS1-R/RPS4 complex, the P68L mutation can be tolerated and this may explain why P68L does not disrupt the interaction between the full-length proteins.

The finding that single amino-acid changes in RRS1-R differentially affect autoimmunity and effector-triggered immunity was somewhat unexpected. This uncoupling of autoimmunity and effector-triggered immunity has never been demonstrated previously in a plant NLR. From this, we can infer that the mechanistic basis of autoimmunity is different from effector-triggered RRS1-R-dependent immunity. There are two prominent theories describing how NLRs switch between ON and OFF states. The original theory states that the NB-ARC domain acts as a molecular switch, via binding of ADP or ATP generating the OFF

and ON states, respectively (Tameling et al., 2002; Tameling et al., 2006; Williams et al., 2011). A modified theory is the equilibrium-based switch activation model, whereby NLRs exist in equilibrium between ADP-bound (OFF) and ATP-bound (ON) and effector binding stabilizes the latter (Bernoux et al., 2016). If either of these apply to the RRS1-R/RPS4 complex, a mutation in RRS1-R^{SLH1} may suppress the switch from ADP-bound to ATP-bound RPS4 through intra- or intermolecular interactions, but perhaps this can be overcome by effector binding. Indeed, immunity triggered by AvrRps4 or PopP2 may simply be stronger than that mediated by auto-active RRS1-R^{SLH1}. Based on the *sushi* mutant morphology, the three mutations that do not affect immunity triggered by AvrRps4 or PopP2 (P68L, G176E or C607Y) are all partial suppressors of the autoimmune phenotype of *slh1*. Conversely, the two mutations that abolish AvrRps4 and PopP2-triggered immunity (C15Y or L816F) fully restore wild-type morphology and thus it can be inferred that they fully suppress *slh1* autoimmunity. Therefore, although P68L, G176E and C607Y mutations at least partially suppress autoimmunity, they may be insufficient to suppress the effector-triggered immune response. Of note, AvrRps4 and PopP2 did not trigger HR in *sushi11* (RRS1-R^{SLH1/G176E}) and *sushi45* (RRS1-R^{SLH1/P68L}) plants despite triggering HR in the *rrs1 rrs1-3* transgenic plants expressing RRS1-R^{SUSHI} in absence of the *slh1* mutation (Fig. S6). We speculate that the presence of the *slh1* mutation in the *sushi* mutants abolished PopP2 recognition capability.

It is notable that there are differences in the mechanistic basis of AvrRps4 and PopP2 recognition (Sarris et al., 2015; Ma et al., 2018). RRS1-R/RPS4 appear to be an exquisitely coevolved NLR pair; whether autoimmunity and effector-triggered immunity can be uncoupled in other NLRs remains to be seen. In this context, it is noteworthy that despite their high degree of similarity, the RRS1-R/RPS4 and RRS1B/RPS4B complexes display major differences in their activation requirements. We showed here that the SH motif in RRS1B is required for AvrRps4 recognition in the tobacco system. However, while this motif is required in the RRS1-R TIR domain to suppress RPS4 TIR domain signaling, it appears that RRS1B TIR domain S22A/H23A can still inhibit this signal. This suggests that the SH motif contributes to activation of the complex in the presence of the effector but not to the repression component maintaining the complex inactive in the absence of an effector. Similarly, the C12Y and P63L changes in the RRS1B TIR domain do not affect the suppression of RPS4 TIR domain-induced cell death.

Outside the TIR-TIR domain interface, the immunocompetence of the RRS1-R/RPS4 complex relies also on physical association between the C-terminal domains of both proteins, specifically the so-called DOM4 of RRS1-R (preceding the WRKY domain) and the CTD of RPS4 (Ma et al., 2018). The presence of the extra Leu residue in the WRKY domain of RRS1-R^{SLH1} likely prevents the inhibition of the complex by DOM4 through disturbed interaction between the WRKY domain and DOM4. We could therefore hypothesize that the L816F mutation situated close to the junction between the LRR domain and DOM4 induced a conformational shift leading to the restoration of the complex inhibition by DOM4 in the presence of the destabilizing extra Leu of the WRKY domain. However, this new conformation may lock the complex in an inactive state that could not be released by binding of the effectors. Further intramolecular interaction studies investigating the role of the LRR domain of RRS1-R for release of the auto-inhibited state and activation of the complex are required to improve our understanding of these mechanisms. Suppression of autoimmunity but maintenance of an immunocompetent complex is, in essence, the default state of all NLRs. The results described herein exemplify the delicate balancing act each NLR must play between auto-inhibition and immunocompetence.

ACKNOWLEDGMENTS

We thank Sylvain Capdevielle and Alice Chin for technical assistance in the early phase of this project. This work was carried out with the support of Next-Generation BioGreen 21 Program (SSAC) of Rural Development Administration (PJ013269), National Research Foundation of Korea (NRF) grant funded by the Korea government (MSIT) (No. 2018R1A5A1023599, SRC) and Australian Research Council (ARC; DP160102244). C.S. is supported by Creative-Pioneering Researchers Program through Seoul National University. S.J.W. is supported by an ARC Discovery Early Career Research Awards (DE160100893). B.K. is a National Health and Medical Research Council (NHMRC) Principal Research Fellow (APP1110971). M.K.H. is supported by Korea Research Fellowship Program through the National Research Foundation of Korea (NRF) funded by the Ministry of Science and ICT (2018H1D3A1A02035413).

AUTHOR CONTRIBUTION

T.E.N., J.L., S.J.W., C.S., K.H.S. designed the study, T.E.N., J.L., S.J.W., S.C., M.K.H., J.Z., C.S. performed the experiments, T.E.N., J.L., S.J.W., S.C., M.K.H., C.S., K.H.S. analysed data, T.E.N., J.L., S.J.W., M.K.H., P.S., B.K., J.D.G.J., C.S., K.H.S wrote the manuscript. TEN & JL contributed equally to this work.

REFERENCES

- Ade J, DeYoung BJ, Golstein C, Innes RW. 2007.** Indirect activation of a plant nucleotide binding site-leucine-rich repeat protein by a bacterial protease. *Proc Natl Acad Sci U S A* **104**(7): 2531-2536.
- Bernoux M, Ve T, Williams S, Warren C, Hatters D, Valkov E, Zhang X, Ellis JG, Kobe B, Dodds PN. 2011.** Structural and functional analysis of a plant resistance protein TIR domain reveals interfaces for self-association, signaling, and autoregulation. *Cell Host Microbe* **9**(3): 200-211.
- Bernoux M, Burdett H, Williams SJ, Zhang X, Chen C, Newell K, Lawrence GJ, Kobe B, Ellis JG, Anderson PA, et al. 2016.** Comparative Analysis of the Flax Immune Receptors L6 and L7 Suggests an Equilibrium-Based Switch Activation Model. *Plant Cell* **28**(1): 146-159.
- Birker D, Heidrich K, Takahara H, Narusaka M, Deslandes L, Narusaka Y, Raymond M, Parker JE, O'Connell R. 2009.** A locus conferring resistance to *Colletotrichum higginsianum* is shared by four geographically distinct Arabidopsis accessions. *Plant J* **60**(4): 602-613.
- Boutrot F, Zipfel C. 2017.** Function, discovery, and exploitation of plant pattern recognition receptors for broad-spectrum disease resistance. *Annu Rev Phytopathol* **55**: 257-286.
- Cesari S, Kanzaki H, Fujiwara T, Bernoux M, Chalvon V, Kawano Y, Shimamoto K, Dodds P, Terauchi R, Kroj T. 2014a.** The NB-LRR proteins RGA4 and RGA5 interact functionally and physically to confer disease resistance. *EMBO J* **33**(17): 1941-1959.
- Cesari S, Bernoux M, Moncuquet P, Kroj T, Dodds PN. 2014b.** A novel conserved

mechanism for plant NLR protein pairs: the ‘integrated decoy’ hypothesis. *Front Plant Sci* **5**: 606.

Clough SJ, Bent AF. 1998. Floral dip: a simplified method for *Agrobacterium*-mediated transformation of *Arabidopsis thaliana*. *Plant J* **16**(6): 735-743.

Cook DE, Mesarich CH, Thomma BP. 2015. Understanding plant immunity as a surveillance system to detect invasion. *Annu Rev Phytopathol* **53**: 541-563.

Deslandes L, Olivier J, Theulieres F, Hirsch J, Feng DX, Bittner-Eddy P, Beynon J, Marco Y. 2002. Resistance to *Ralstonia solanacearum* in *Arabidopsis thaliana* is conferred by the recessive RRS1-R gene, a member of a novel family of resistance genes. *Proc Natl Acad Sci U S A* **99**(4): 2404-2409.

Dodds PN, Lawrence GJ, Catanzariti AM, Teh T, Wang CI, Ayliffe MA, Kobe B, Ellis JG. 2006. Direct protein interaction underlies gene-for-gene specificity and coevolution of the flax resistance genes and flax rust avirulence genes. *Proc Natl Acad Sci U S A* **103**(23): 8888-8893.

Engler C, Kandzia R, Marillonnet S. 2008. A one pot, one step, precision cloning method with high throughput capability. *PLoS One* **3**(11): e3647.

Frost D, Way H, Howles P, Luck J, Manners J, Hardham A, Finnegan J, Ellis J. 2004. Tobacco transgenic for the flax rust resistance gene L expresses allele-specific activation of defense responses. *Mol Plant Microbe Interact* **17**(2): 224-232.

Johnson KC, Dong OX, Huang Y, Li X. 2012. A rolling stone gathers no moss, but resistant plants must gather their moses. *Cold Spring Harb Symp Quant Biol* **77**: 259-268.

Jones JD, Dangl JL. 2006. The plant immune system. *Nature* **444**(7117): 323-329.

Le Roux C, Huet G, Jauneau A, Camborde L, Trémousaygue D, Kraut A, Zhou B, Levaillant M, Adachi H, Yoshioka H, et al. 2015. A receptor pair with an integrated decoy converts pathogen disabling of transcription factors to immunity. *Cell* **161**(5): 1074-1088.

Lee SK, Song MY, Seo YS, Kim HK, Ko S, Cao PJ, Suh JP, Yi G, Roh JH, Lee S, et al. 2009. Rice Pi5-mediated resistance to *Magnaporthe oryzae* requires the presence of

two coiled-coil-nucleotide-binding-leucine-rich repeat genes. *Genetics* **181**(4): 1627-1638.

- Li X, Clarke JD, Zhang Y, Dong X. 2001.** Activation of an EDS1-mediated R-gene pathway in the *snc1* mutant leads to constitutive, NPR1-independent pathogen resistance. *Mol Plant Microbe Interact* **14**(10): 1131-1139.
- Ma Y, Guo H, Hu L, Martinez PP, Moschou PN, Cevik V, Ding P, Duxbury Z, Sarris PF, Jones JDG. 2018.** Distinct modes of derepression of an Arabidopsis immune receptor complex by two different bacterial effectors. *Proc Natl Acad Sci U S A* (doi/10.1073/pnas.1811858115)
- Narusaka M, Shirasu K, Noutoshi Y, Kubo Y, Shiraishi T, Iwabuchi M, Narusaka Y. 2009.** RRS1 and RPS4 provide a dual Resistance-gene system against fungal and bacterial pathogens. *Plant J* **60**(2): 218-226.
- Nishimura MT, Anderson RG, Cherkis KA, Law TF, Liu QL, Machius M, Nimchuk ZL, Yang L, Chung EH, El Kasmi F, et al. 2017.** TIR-only protein RBA1 recognizes a pathogen effector to regulate cell death in Arabidopsis. *Proc Natl Acad Sci U S A* **114**(10): E2053-E2062.
- Noutoshi Y, Ito T, Seki M, Nakashita H, Yoshida S, Marco Y, Shirasu K, Shinozaki K. 2005.** A single amino acid insertion in the WRKY domain of the Arabidopsis TIR-NBS-LRR-WRKY-type disease resistance protein SLH1 (sensitive to low humidity 1) causes activation of defense responses and hypersensitive cell death. *Plant J* **43**(6): 873-888.
- Sarris PF, Duxbury Z, Huh SU, Ma Y, Segonzac C, Sklenar J, Derbyshire P, Cevik V, Rallapalli G, Saucet SB, et al. 2015.** A plant immune receptor detects pathogen effectors that target WRKY transcription factors. *Cell* **161**(5): 1089-1100.
- Saucet SB, Ma Y, Sarris PF, Furzer OJ, Sohn KH, Jones JD. 2015.** Two linked pairs of Arabidopsis TNL resistance genes independently confer recognition of bacterial effector AvrRps4. *Nat Commun* **6**: 6338.
- Schreiber KJ, Bentham A, Williams SJ, Kobe B, Staskawicz BJ. 2016.** Multiple domain associations within the Arabidopsis immune receptor RPP1 regulate the activation of programmed cell death. *PLoS Pathog* **12**(7): e1005769.

- Sohn KH, Segonzac C, Rallapalli G, Sarris PF, Woo JY, Williams SJ, Newman TE, Paek KH, Kobe B, Jones JD. 2014.** The nuclear immune receptor RPS4 is required for RRS1SLH1-dependent constitutive defense activation in *Arabidopsis thaliana*. *PLoS Genet* **10**(10): e1004655.
- Swiderski M, Birker D, Jones JDG. 2009.** The TIR domain of TIR-NB-LRR resistance proteins is a signaling domain involved in cell death induction. *Mol Plant Microbe Interact* **22**: 157-165.
- Takken F, Tameling W. 2009.** To nibble at plant resistance proteins. *Science* **324**(5928): 744.
- Tameling WI, Elzinga SD, Darmin PS, Vossen JH, Takken FL, Haring MA, Cornelissen BJ. 2002.** The tomato R gene products I-2 and MI-1 are functional ATP binding proteins with ATPase activity. *Plant Cell* **14**(11): 2929-2939.
- Tameling WI, Vossen JH, Albrecht M, Lengauer T, Berden JA, Haring MA, Cornelissen BJ, Takken FL. 2006.** Mutations in the NB-ARC domain of I-2 that impair ATP hydrolysis cause autoactivation. *Plant Physiol* **140**(4): 1233-1245.
- Thomas WJ, Thireault CA, Kimbrel JA, Chang JH. 2009.** Recombineering and stable integration of the *Pseudomonas syringae* pv. *syringae* 61 hrp/hrc cluster into the genome of the soil bacterium *Pseudomonas fluorescens* Pf0-1. *Plant J* **60**(5): 919-928.
- Wan L, Zhang X, Williams SJ, Ve T, Bernoux M, Sohn KH, Jones JD, Dodds PN, Kobe B. 2013.** Crystallization and preliminary X-ray diffraction analyses of the TIR domains of three TIR-NB-LRR proteins that are involved in disease resistance in *Arabidopsis thaliana*. *Acta Crystallogr Sect F Struct Biol Cryst Commun* **69**(Pt 11): 1275-1280.
- Wiedemann C, Bellstedt P, Gorlach M. 2013.** CAPITO--a web server-based analysis and plotting tool for circular dichroism data. *Bioinformatics* **29**(14): 1750-1757.
- Williams SJ, Sornaraj P, deCourcy-Ireland E, Menz RI, Kobe B, Ellis JG, Dodds PN, Anderson PA. 2011.** An autoactive mutant of the M flax rust resistance protein has a preference for binding ATP, whereas wild-type M protein binds ADP. *Mol Plant Microbe Interact* **24**(8): 897-906.

Williams SJ, Sohn KH, Wan L, Bernoux M, Sarris PF, Segonzac C, Ve T, Ma Y, Saucet SB, Ericsson DJ. 2014. Structural basis for assembly and function of a heterodimeric plant immune receptor. *Science* **344**(6181): 299-303.

Zhang X, Dodds PN, Bernoux M. 2017a. What do we know about NOD-like receptors in plant immunity? *Annu Rev Phytopathol* **55**: 205-229.

Zhang X, Bernoux M, Bentham AR, Newman TE, Ve T, Casey LW, Raaymakers TM, Hu J, Croll TI, Schreiber KJ, et al. 2017b. Multiple functional self-association interfaces in plant TIR domains. *Proc Natl Acad Sci U S A* **114**(10): E2046-E2052.

Zhang Y, Dorey S, Swiderski M, Jones JD. 2004. Expression of RPS4 in tobacco induces an AvrRps4- independent HR that requires EDS1, SGT1 and HSP90. *Plant J* **40**(2): 213-224.

Zhang Y, Goritschnig S, Dong X, Li X. 2003. A gain-of-function mutation in a plant disease resistance gene leads to constitutive activation of downstream signal transduction pathways in suppressor of npr1-1, constitutive 1. *Plant Cell* **15**(11): 2636-2646.

TABLES

Table 1 *RRS1-R* intragenic mutations identified in *sushi*.

<i>sushi</i> ^a	Genomic ^b	Exon ^c	Domain ^d	Protein ^e
84	tGc>tAc	1	TIR	C15Y
40	Cga>Tga	1	TIR	R33*
45	cCc>cTc	1	TIR	P68L
81	Cga>Tga	2	NB-ARC	R151*
11	gGa>gAa	2	NB-ARC	G176E
33	tGg>tAg	2	NB-ARC	W178*
78	tGg>tAg	3	NB-ARC	W441*
26	tGc>tAc	4	LRR	C607Y
23	cCa>cTa	4	LRR	P741L
85	Caa>Taa	4	LRR	Q787*
61	Cga>Tga	4	LRR	R800*
88	Ctt>Ttt	4	LRR	L814F

^aNumber of the sequenced *sushi* line.

^bNucleotide mutation identified in *RRS1-R* codon.

^cLocalization of the mutation in *RRS1-R* CDS.

^dLocalization of the mutation in *RRS1-R* conserved domain.

^eResulting amino acid change in *RRS1-R* protein (* indicates STOP codon).

FIGURE LEGENDS

Fig. 1 Phenotype of the *sushi* lines carrying missense mutations in the *RRS1-R^{SLH1}* gene. (a) Morphology of *sushi* carrying mutations in the *RRS1-R^{SLH1}* gene (M3 generation), wild type No-0 and *slh1* plants grown at 22°C under short-day condition for 5 weeks. Scale bar represents 1 cm. (b) qRT-PCR analysis of selected *RRS1-R^{SLH1}*-regulated genes in wild-type No-0, *slh1* and *sushi* lines carrying mutations in the *RRS1-R^{SLH1}* gene. Transcript accumulation is presented relative to wild-type No-0. Plants were grown at 28°C for 5 weeks then shifted to 19°C for 4 days prior to total RNA isolation. Expression values represent the mean \pm SE of the mean measured in each genotype from one representative experiment out of three biological repeats.

Fig. 2 Identification of 5 missense mutations in the *RRS1-R* gene that caused suppression of *slh1* lethality. (a) The F₁ hybrids between *Ws-2 rrs1-1* and *sushi* were grown for 5 weeks at 22°C under short-day condition before the photograph was taken. Scale bar represents 1 cm. (b) Morphological phenotype of F₁ hybrids (shown in (a)) correlates with *FMO1*, *PBS3* and *PR1* transcript level as determined by qRT-PCR. Transcript accumulation is presented relative to the No-0 \times *rrs1-1* F₁ hybrid. Expression values represent the mean \pm SE of the mean measured in each genotype from one representative experiment out of two biological repeats.

Fig. 3 Several *SUSHI* mutations in *RRS1-R^{SLH1}* that abolish autoimmunity are not required for effector-triggered immunity. (a) Expression of the *RRS1-R^{SUSHI}* variants in transgenic *rrs1-3 rrs1B-1 (rrs1 rrs1B)* T2 lines as determined by semi-quantitative PCR. (b) Analysis of AvrRps4- or PopP2-triggered hypersensitive response in *rrs1 rrs1B* transgenic lines expressing *RRS1-R^{SUSHI}* variants. Five-week-old Arabidopsis leaves were infiltrated with Pf0-1(T3S) strains carrying empty vector (EV), *avrRps4* or *popP2*. The photograph was taken at 24 hours post-infiltration (hpi). (c) Restriction of pathogen growth in *rrs1 rrs1B* transgenic lines expressing *RRS1-R^{SUSHI}* variants. Five-week-old Arabidopsis leaves were infiltrated with *Pseudomonas syringae* pv. *tomato (Pto)* DC3000 carrying EV, *avrRps4* or *popP2*. Infected leaf samples were taken at 4 d post-infiltration (dpi) to measure bacterial numbers. The results presented are the mean and \pm SE of the number of colonies recovered. Asterisks

indicate statistical difference at the 95% confidence level based on Student's *t*-test between selected sample and EV for the same genotype. Data presented are from one representative experiment out of 3 biological repeats conducted on two independent T2 lines for each genotype.

Fig. 4 The C15Y mutation significantly reduces RRS1-R interaction with RPS4. Full-length wild-type (WT), C15Y, P68L, G176E, C607Y, P741L and L816F variants of RRS1-R, C-terminally tagged with 3xFLAG, were transiently co-expressed with full-length RPS4 C-terminally fused with 6xHA tag in *Nicotiana benthamiana*. Total protein extracts were subjected to anti-FLAG immunoprecipitation (IP) before immunoblotting (IB) with anti-FLAG or anti-HA antibodies. Ponceau staining attests equal loading. This experiment was conducted twice with similar results.

Fig. 5 C15Y or P68L mutations in RRS1-R TIR domain cause suppression of RPS4 TIR domain-induced cell death and loss of interaction with RPS4 TIR domain. (a) Structure of RRS1-R (orange)-RPS4 (teal) TIR domain complex (PDB ID 4CST) shown in cartoon representation. Residues important in this study are shown in stick representation and labelled. (b) The RRS1-R(1-175) TIR domain wild type (WT), S25A/H26A (SH-AA), C15Y or P68L variants were co-expressed with GFP or with the RPS4(1-236) TIR domain. RPS4 TIR domain-induced cell death was photographed at 3 d after agro-infiltration (upper panel). Dotted boxes indicate agro-infiltrated leaf area showing cell death. Occurrence of cell death on the total number of infiltrated areas across 3 biological repeats is indicated. Expression of RRS1-R(1-175) protein variants in tobacco cells (lower panel) was assayed by immunoblotting (IB) with anti-FLAG antibodies (c) RRS1-R(1-175)^{C15Y} and RRS1-R(1-175)^{P68L} do not interact strongly with RPS4(1-236) when co-expressed in yeast cells (upper panel). Expression of RRS1-R(1-175) protein variants in yeast cells (lower panel) was assayed with anti-HA antibodies. (d) Circular dichroism spectra of purified RRS1-R(1-175)^{WT} and RRS1-R(1-175)^{C15Y} protein variants. (e) Coomassie stained SDS-PAGE of purified proteins used in the protein-protein interaction assays. (f) Protein-protein interaction analysis. The elution profiles represent the UV280 nm protein trace of purified proteins separated by size exclusion chromatography.

Fig. 6 The *SUSHI* mutations in RRS1B TIR domain do not affect AvrRps4 recognition. (a) The RRS1-R^{C15Y} variant cannot recognize AvrRps4 when co-expressed with RPS4 in *Nicotiana tabacum*. Full-length wild type (WT), S25A/H26A (SH-AA), C15Y or P68L RRS1-R variants were co-expressed with RPS4 and AvrRps4 in *N. tabacum* leaf cells. (b) The RRS1B^{C12Y} variant recognizes AvrRps4 when co-expressed with RPS4B in *N. tabacum*. Full-length wild type (WT), S22A/H23A (SH-AA), C12Y or P63L RRS1B variants were co-expressed with RPS4B and AvrRps4 in *N. tabacum* leaf cells. (c) The SH motif in the RRS1B TIR domain is not required to suppress RPS4 TIR domain-mediated cell death. Wild type (WT), S22A/H23A (SH), C12Y or P63L RRS1B(1-166) TIR domain variants were co-expressed with GFP or RPS4(1-236). All photographs were taken 3 days after agro-infiltration. Dotted boxes indicate cell death. Occurrence of cell death on the total number of infiltrated areas across 3 biological repeats is indicated.

Supporting Information

Fig. S1 CAPS marker analysis in *sushi* x *rrs1-1* F₁ hybrids to test *sh1* heterozygosity.

Fig. S2 Alignment of *RRS1* allele sequence and *SUSHI* mutations in No-0, Col-0 and Ws-2 Arabidopsis ecotypes.

Fig. S3 Multiple alignment of RRS1-R (No-0 and Ws-2) and RRS1B TIR domains.

Fig. S4 Protein expression analysis of RRS1B variants in *N. benthamiana*.

Fig. S5 Structural view of the C15Y mutation in RRS1-R TIR domain.

Fig. S6 PopP2 recognition in *sushi* mutants.

Table S1 List of the primers used in this study.

Figure 1

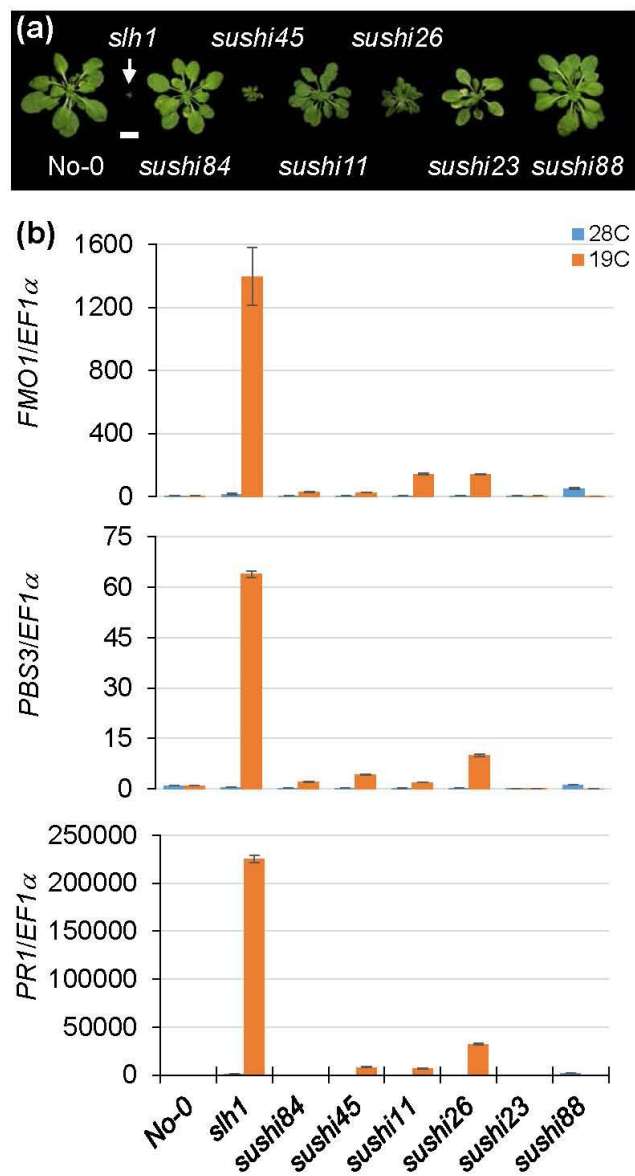


Figure 2

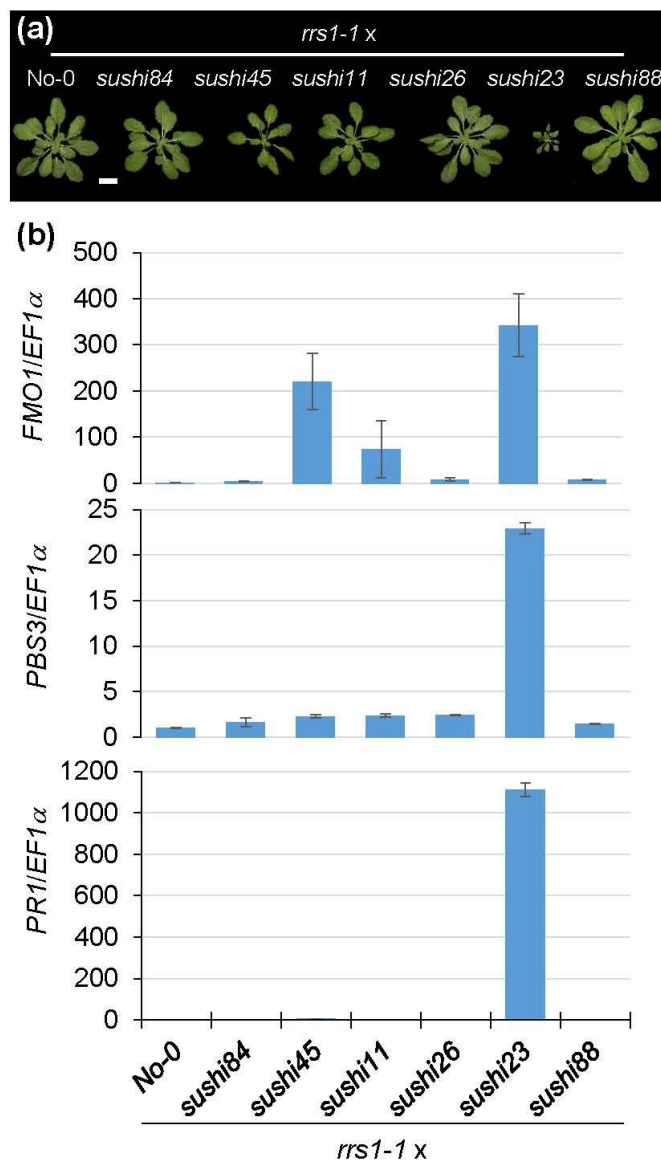


Figure 3

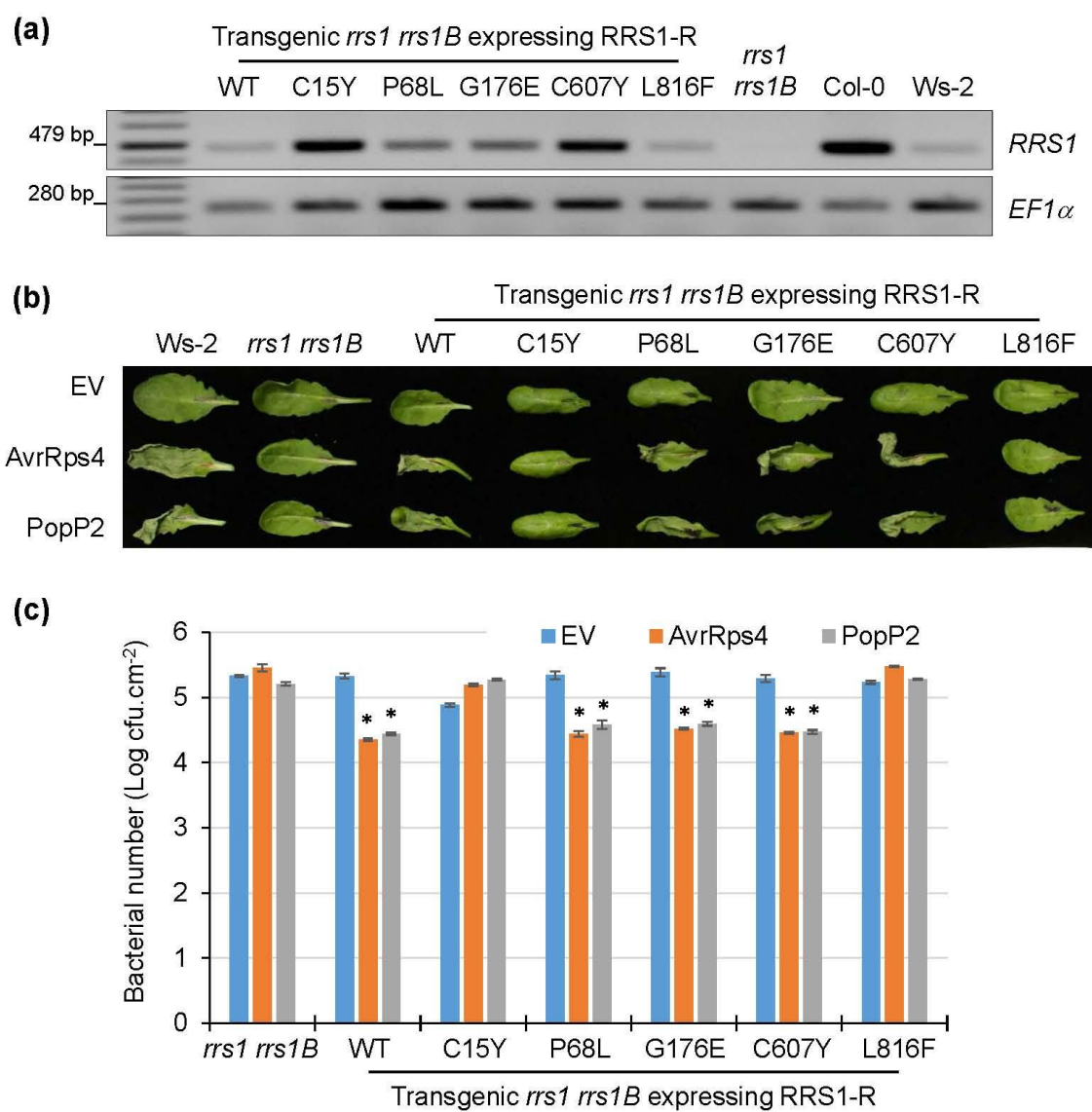


Figure 4

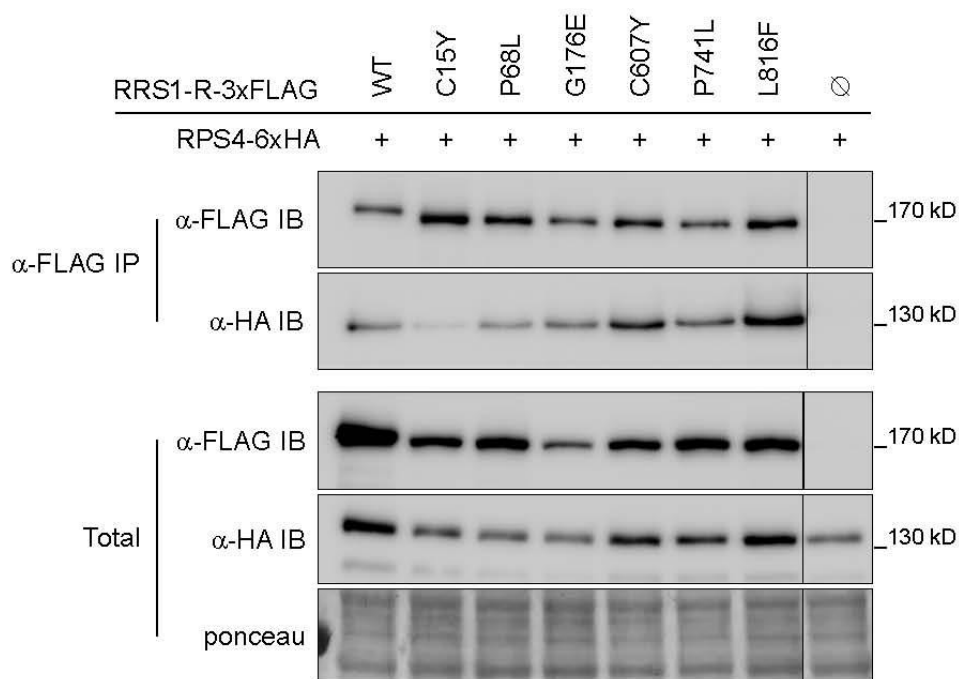


Figure 5

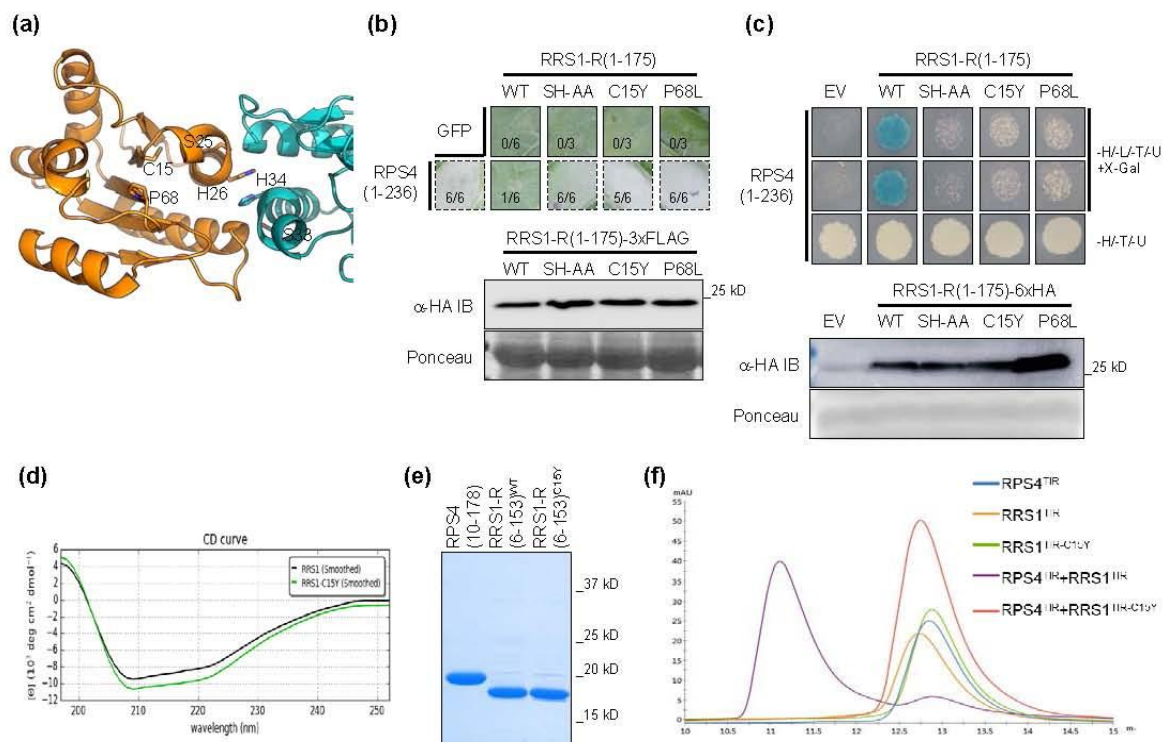


Figure 6

